

BBA 76577

ANOMALOUS TRANSPORT KINETICS AND THE GLUCOSE CARRIER HYPOTHESIS

DAVID M. REGEN and HAROLD L. TARPLEY

Physiology Department, Vanderbilt University, School of Medicine, Nashville, Tenn. 37232 (U.S.A.)

(Received September 3rd, 1973)

SUMMARY

In recent years several observations of glucose transport in human erythrocytes have been difficult to explain by the carrier model. Three new models have been described as candidates to supplant the carrier hypothesis. In this paper, some of the anomalous findings of Miller ((1968) *Biophys. J.* 8, 1329–1338) and of Stein's group ((1972) *Biochim. Biophys. Acta* 266, 161–173; (1966) *Biochim. Biophys. Acta* 127, 179–193) are discussed in terms of the carrier model with and without unstirred layers (unstirred layers being diffusion barriers between the carrier and the bulk aqueous phases inside and outside the cell). The carrier model with no simplifying assumptions (Regen, D. M. and Morgan, H. E. (1964) *Biochim. Biophys. Acta* 79, 151–166) with the addition of unstirred layers suggested by Miller, accommodates virtually all the data which have been considered grounds for its rejection. All transport constants for glucose and galactose are evaluated, including the diffusion constants in the unstirred layers. Some novel ways of interpreting kinetic data are described. The asymmetric features of the carrier described by Geck are confirmed ((1971) *Biochim. Biophys. Acta* 241, 462–472).

INTRODUCTION

Prior to 1964 there were few observations on glucose transport in human erythrocytes which were not predicted by the simple mobile-carrier hypothesis of Widdas [1] and of Rosenberg and Wilbrandt [2]. It appeared for example that rates of glucose entry and of exit were not equal under circumstances where they should have been [3, 4]. However, the experimental techniques and data analyses were subject to considerable error. The discrepancies between predicted and observed behavior were explained in this manner [4, 5], and there were no compelling reasons to introduce a more complex mechanism or a more complex kinetic treatment of the carrier mechanism. Nevertheless, Regen and Morgan [5] derived equations from the carrier model using a minimum of simplifying assumptions. In particular, it was not assumed that decomposition of the sugar-carrier complex is much faster than its translocation, nor was it assumed that the unloaded and loaded carriers move with equal facility inward or outward. The analysis showed what would be expected

if the simplifying assumptions used by others were not valid — that the maximal rates of entry, exit and equilibrium exchange of a sugar would not be the same; the concentration of the sugar needed for a half-maximal entry, exit and exchange would not be the same; but the ratio, V/K_m , for each of these experiments would be the same. Moreover, the flux ratio and counterflow effects would reveal yet another constant related to K_m but different, if the simplifying assumptions were wrong. Using the rabbit erythrocyte, where sugar transport is slow enough to allow rate measurements by ordinary methods, Regen and Morgan [5] carried out all of these experiments to determine the validity of the simplifying assumptions. The results showed these assumptions to be entirely valid for the rabbit cell [5]. Subsequently, Levine et al. [6] and Mawe and Hempling [7] showed that the maximal rate of glucose exchange in the human erythrocyte is faster than the maximal rate of exit, i.e. that external glucose promotes efflux of inside glucose. The latter was interpreted [6] according to a simplified version of our kinetic analysis [5] to mean that exit is limited by return of the free carrier to the inside and that the carrier loaded from the outside moves to the inside more readily than does the free carrier. Thus, glucose moving in increases the carrier available on the inside to participate in efflux. Later Miller [8] observed the same phenomenon but offered a new explanation [9]. He suggested that exit is limited somewhat by diffusion from the external surface to the bulk external medium. Thus, sugar molecules released at the external surface stand a good chance of getting back on the carrier and returning to the inside. The exchange of labelled internal sugar for unlabelled external sugar is much faster than exit, since the unlabelled sugar on the outside will competitively inhibit this re-entry of labelled sugar. He repeated several observations of other workers which were not predicted by the simplified carrier kinetics. He could explain several of the anomalies in terms of the diffusion barrier (unstirred layer). However, he stated that he could not fit all of his data to his model, which included the simplified carrier assumptions with the diffusion events on either side of the membrane. Naftalin [10] later provided support for the kinetic significance of diffusion from the membrane by showing that increased mixing accelerated exit and exchange, exit being accelerated by a larger factor. Recently Geck [11] attempted to fit the various observations of Miller [8] and the more recent observations of Lacko, et al. [12] to the carrier model without the simplifying assumption of equal mobilities of loaded and unloaded carrier in either direction. In essence, he returned to the original interpretation given to these phenomena [5]. His treatment included no unstirred layer, yet he managed to fit most though not all of the data. In summary, then, a satisfactory explanation of all anomalous observations on the basis of the mobile carrier hypothesis has not been provided. As a consequence, several new models have been devised which purported to accommodate most findings [13–16]. The carrier model, if it also can accommodate the data, should not be discarded in favor of a more complex [13] or chemically less probable [14] hypothesis.

RESULTS

Model

Fig. 1 shows the carrier model essentially as we considered it earlier but with diffusion steps on either side of the membrane. Here, the movement of loaded car-

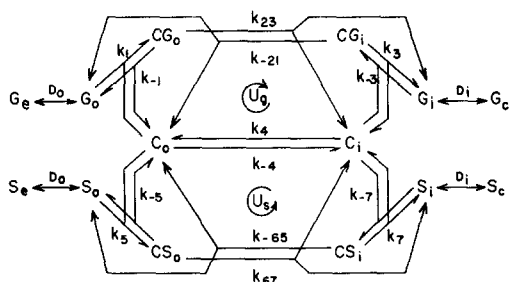


Fig. 1. Model of glucose carrier with an unstirred layer over each membrane interface. See accompanying text for symbol definitions. Reaction constants associated with carrier-glucose complex bear subscripts with digits 1, 2 and/or 3. The reaction constants having digits 5, 6 and/or 7 are concerned with carrier-sugar (other than glucose) complex. In the earlier presentation of this model [5] the assignment of these subscripts was the other way around. The translocation of free carrier (k_4 and k_{-4}) is a step common to any sugar present. Subscripts are positive for reactions in the direction of sugar uptake, negative for reactions in the opposite direction. Another difference between this presentation and the earlier one [5] is that CG_o symbolizes all carrier-glucose complexes (regardless of location) which were formed by collision of C_o and G_o . Likewise CG_i symbolizes all carrier-glucose complexes (regardless of location) formed by collision of C_i and G_i . This means that the conversion of CG_o to $C_i + G_i$ is treated as a single event with rate constant k_{23} ; and conversion of CG_i to C_o and G_o is treated as a single event with rate constant k_{-21} . This greatly simplifies the algebra, but involves no assumptions about rate-limiting steps. It is recognized that CG formed on the outside by collision of C_o and G_o will have passed through any number of stages between formation and release of glucose on the inside, and that the last stage may be identical in location and conformation to the CG immediately formed by collision of C_i and G_i ; but, in the steady-state, the fraction of CG_o in any stage will bear a constant ratio to that in any other stage. Hence, the stages of CG_o are kinetically insensible and can be grouped together as a single entity, CG_o . This is the same treatment given to the "central complex" in steady-state enzyme kinetics. The coefficient k_{23} is the fraction of CG_o undergoing decomposition on the inside each minute; k_{-1} is the fraction of CG_o undergoing decomposition on the outside each minute. The other constants can be understood by analogy or are self-explanatory.

rier across the membrane followed by the release of sugar is treated as a single event. The symbolism is as follows:

- G = a sugar (in this paper, glucose);
- S = another sugar which may or may not be present (in this paper, galactose);
- C = carrier;
- o = outside interface;
- i = inside interface;
- e = bulk external medium;
- c = bulk cell fluid;
- D = diffusion constant for movement between interfaces and bulk volumes;
- k = rate constant for transport event.

All kinetic features of this system can be readily derived from Eqn 1, showing the effects of two sugars (G and S), present at substantial concentrations, on the entry of a sugar, X, which may be either G, S, labelled G, labelled S, or a third sugar present at minute concentration relative to its Michaelis constants and related constants. This equation was derived by the approach described earlier [5] and is much like Eqn 14 published by Geck [11]. The positive numerator term divided by

the denominator is influx, U_{x+} ; the negative numerator term divided by the denominator is efflux, U_{x-} . The satellite equations define the symbols and take the unstirred layers into account.

$$U_x = \frac{F_x([X_o](1 + [G_i]/R_g + [S_i]/R_s) - [X_i](1 + [G_o]/R_g + [S_o]/R_s))}{1 + \frac{[G_o]}{K_{go}} + \frac{[G_i]}{K_{gi}} + \frac{[G_o][G_i]}{R_g B_g} + \frac{[S_o]}{K_{so}} + \frac{[S_i]}{K_{si}} + \frac{[S_o][S_i]}{R_s B_s} + \frac{[G_o][S_i]}{N_{gs}} + \frac{[S_o][G_i]}{N_{sg}}} \quad (1)$$

U_x = rate of X entry;

$[X_o]$ = concn X at outside surface = $[X_e] - U_x/D_o$;

$[X_i]$ = concn X at inside surface = $[X_e] + U_x/D_i$;

$[G_o]$ = concn G at outside surface = $[G_e] - U_g/D_o$;

$[G_i]$ = concn G at inside surface = $[G_e] + U_g/D_i$;

$[S_o]$ = concn S at outside surface = $[S_e] - U_s/D_o$;

$[S_i]$ = concn S at inside surface = $[S_e] + U_s/D_i$;

F_x = activity constant for X transport = V/K_m for X transport.

$$\text{If } X = G, \text{ then } F_x = F_g = C_t \frac{k_4}{k_4 + k_{-4}} \cdot \frac{k_1 k_{23}}{k_{-1} + k_{23}} = C_t \frac{k_{-4}}{k_4 + k_{-4}} \cdot \frac{k_{-3} k_{-21}}{k_3 + k_{-21}} \quad (2)$$

$$R_g = \text{flux-ratio constant for G} = \frac{k_{-4}(k_{-1} + k_{23})}{k_1 k_{23}} = \frac{k_4(k_3 + k_{-21})}{k_{-3} k_{-21}} \quad (3)$$

$$K_{go} = \text{Michaelis constant for G entry} = \frac{k_{-1} + k_{23}}{k_1} \cdot \frac{k_4 + k_{-4}}{k_4 + k_{23}} \quad (4)$$

$$K_{gi} = \text{Michaelis constant for G exit} = \frac{k_3 + k_{-21}}{k_{-3}} \cdot \frac{k_4 + k_{-4}}{k_{-4} + k_{-21}} \quad (5)$$

$$B_g = \text{half maximal constant for G exchange; } 1/B_g = 1/K_{go} + 1/K_{gi} - 1/R_g \quad (6)$$

$$\text{If } X = S, \text{ then } F_x = F_s = C_t \frac{k_4}{k_4 + k_{-4}} \cdot \frac{k_5 k_{67}}{k_{-5} + k_{67}} = C_t \frac{k_{-4}}{k_4 + k_{-4}} \cdot \frac{k_{-7} k_{-65}}{k_7 + k_{-65}} \quad (2a)$$

$$R_s = \text{flux ratio or counterflow constant for S} = \frac{k_{-4}(k_{-5} + k_{67})}{k_5 k_{67}} = \frac{k_4(k_7 + k_{-65})}{k_{-7} k_{-65}} \quad (3a)$$

$$K_{so} = \text{Michaelis constant for S entry} = \frac{k_{-5} + k_{67}}{k_5} \cdot \frac{k_4 + k_{-4}}{k_4 + k_{67}} \quad (4a)$$

$$K_{si} = \text{Michaelis constant for S exit} = \frac{k_7 + k_{-65}}{k_{-7}} \cdot \frac{k_4 + k_{-4}}{k_{-4} + k_{-65}} \quad (5a)$$

$$B_s = \text{half maximal constant for S exchange; } 1/B_s = 1/K_{so} + 1/K_{si} - 1/R_s \quad (6a)$$

$$1/N_{gs} = 1/K_{go}R_s + 1/K_{si}R_g - 1/R_gR_s \quad (7)$$

$$1/N_{sg} = 1/K_{so}R_g + 1/K_{gi}R_s - 1/R_gR_s \quad (8)$$

Eqn 1 is appropriate for the most complicated experimental conditions encountered in the literature. Most experiments are so designed that several terms may be dropped and constants in the other terms evaluated. However, the possibility of unstirred layers greatly limits the degree to which experimental design can simplify interpretation.

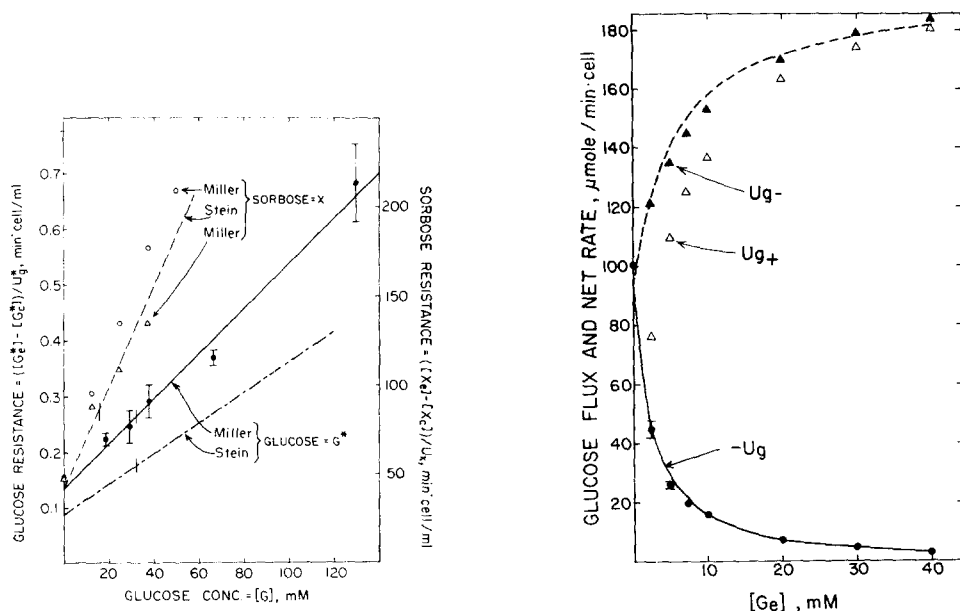


Fig. 2. Effects of glucose at equilibrium on the resistance to glucose exchange (●) and the resistance to sorbose transport (○, △). All the points are from data reported by Miller [8]. The solid line is intended to fit Miller's glucose-exchange data (●). The dot-dash line represents the results of Eilam and Stein [17] and agrees well with Miller's data with respect to the concentration of glucose (32 mM) which doubles resistance to glucose exchange, but not with respect to the minimum resistance. Since Miller used optical measurements for his sorbose transport studies, his only reliable point is that in the absence of glucose (minimum resistance). According to Levine and Stein [18] the concentrations of glucose which double sorbose resistance (estimated by [^{14}C] sorbose transport with sorbose concentration 2 or 20 mM) are 13 mM at 25 °C and 19 mM at 13 °C. Interpolation by Van't Hoff plot indicates that this concentration should be 15.1 mM at 20 °C. However, these workers provide no information on the actual sorbose transport rates; and the dashed line showing resistance doubling at 15.1 mM was arbitrarily made to intercept 10 % below the minimum resistance indicated by Miller, on the assumption that the 230 mM sorbose (used by Miller) might bind about 10 % of the carrier and increase its own resistance by this fraction. This refinement plays no role in the outcome of the kinetic analysis. The fact that Miller's sorbose data also show a doubling of resistance at nearly the same glucose concentration (13 mM) is surprising, since the counter movements of glucose would have interfered with his optical estimates of sorbose transport.

Fig. 3. Glucose exit (●), glucose efflux (▲) and glucose influx (△) in cells loaded with about 130 mM glucose and various external glucose concentrations. The glucose exit data are those of Miller [8] and should be very dependable. The efflux data are an approximation (described in the text) based on the results of Naftalin [10] under conditions somewhat different from those of Miller. All subsequent calculations based on these data take account of osmotic swelling by use of the formula $[G_c] = G_c(310 + [G_e]) / (310 + G_c)$, where G_c in $\mu\text{moles/cell}$ is the cell glucose content. The solid line through the exit data corresponds to the solid line in Fig. 5. The dash line shows the efflux predicted by the constants obtained from the solid line of Fig. 5.

Glucose exchange and inhibition of sorbose transport

Fig. 2 shows a plot of glucose-exchange resistance with several concentrations of glucose at equilibrium, as observed by Miller [8] and by Eilam and Stein [17]. It also shows sorbose entry and exit resistances as affected by several concentrations of glucose at equilibrium [8, 18]. Since only glucose, G, was present in substantial amounts (relative to dissociation constant), all the S terms in Eqn 1 are zero. Since $[G_o] = [G_i]$ and $U_g = 0$, the denominator reduced to $(1 + [G]/B_g)(1 + [G]/R_g)$, the second factor then cancelling the similar factor in the numerator, leaving the simpler equation:

$$U_x = \frac{F_x([X_o] - [X_i])}{1 + [G]/B_g} = \frac{F_x((X_e) - U_x/D_o) - ([X_e] + U_x/D_i)}{1 + [G]/B_g} \quad (9)$$

The transport resistance offered by the membrane is given by:

$$\frac{[X_o] - [X_i]}{U_x} = \frac{1}{F_x} + [G] \frac{1}{F_x B_g} \quad (9a)$$

The transport resistance of the membrane and unstirred layers is:

$$\frac{[X_e] - [X_c]}{U_x} = \frac{1}{F_x} + \frac{1}{D_o} + \frac{1}{D_i} + [G] \frac{1}{F_x B_g} \quad (9b)$$

From the intercept and slope of Miller's glucose-exchange data [8] we can make the following estimates of glucose constants*: the minimum transport resistance is $1/D_o + 1/D_i + 1/F_g = 0.133 \text{ min} \cdot \text{cell} \cdot \text{ml}^{-1}$; the V for exchange is $F_g B_g = 247 \mu\text{moles} \cdot \text{min}^{-1} \cdot \text{cell}^{-1}$. From the intercept and slope of Levine and Stein's sorbose data [18] (the dashed line) we have: $1/D_o + 1/D_i + 1/F_x = 43 \text{ min} \cdot \text{cell} \cdot \text{ml}^{-1}$; $F_x B_g = 0.351 \mu\text{mole} \cdot \text{min}^{-1} \cdot \text{cell}^{-1}$. By combining the above information: resistance by the combined unstirred layers is $1/D_o + 1/D_i = 0.072 \text{ min} \cdot \text{cell} \cdot \text{ml}^{-1}$, which is half the minimal resistance to glucose but only a tiny fraction of the resistance to sorbose; $F_g = 16.38 \text{ ml} \cdot \text{min}^{-1} \cdot \text{cell}^{-1}$; $F_x = 0.0233 \text{ ml} \cdot \text{min}^{-1} \cdot \text{cell}^{-1}$; $B_g = 15.07 \text{ mM}$.

Flux Ratio

According to Miller [8], efflux of glucose from cells containing 130 mM glucose into sugar-free medium is $100 \mu\text{moles} \cdot \text{min}^{-1} \cdot \text{cell}^{-1}$. The addition of 130 mM glucose to the medium raises this efflux to $197 \mu\text{moles} \cdot \text{min}^{-1} \cdot \text{cell}^{-1}$ as shown in Fig. 2 (Miller's glucose resistance line). Judging from Naftalin's observations [10] with well-stirred cells, the dependency of efflux on external glucose is hyperbolic and shows a K_m of 10 mM. From these data, we can calculate roughly the effluxes that Miller [8] might have observed** in his exit experiments had he made the measure-

* The word "cell" in the dimensions refers to the number of cells which, if equilibrated with sugar under isotonic conditions, would contain the amount of sugar in 1 ml extracellular fluid. This is 1/1000 of the "cell unit" described by others [8].

** Although Miller's efflux data [8] agreed with those observed by Naftalin [10] in poorly stirred cells, the stirring procedure described by Miller is considered very effective [19, 20]. We, therefore, assume the lower half-excision concentration of 10 rather than the 25 mM seen in poorly stirred cells.

ments: $U_{g-} = 100 + 105[G_e]/(10 + [G_e])$. This gives $U_{g-} = 197 \mu\text{moles} \cdot \text{min}^{-1} \cdot \text{cell}^{-1}$ at $[G_e] = 130 \text{ mM}$. With this expression and exit data of Miller, one can calculate influx: $U_{g+} = U_g + U_{g-}$. Therefore, U_{g+} and U_{g-} can be calculated at several external glucose concentrations. Fig. 3 shows the exit data of Miller and the fluxes calculated from Naftalin's observations.

The flux-ratio equation involves only the numerator of Eqn 1, the denominator cancelling. If $[S_o] = [S_i] = 0$ then the flux ratio [5] at the membrane is:

$$\frac{U_{x+}}{U_{x-}} = \frac{[X_o]}{[X_i]} \cdot \frac{R_g + [G_i]}{R_g + [G_o]} \quad (10)$$

The flux ratio across unstirred layers and membrane together is only slightly more complex:

$$\frac{U_{x+}}{U_{x-}} = \frac{[X_e]}{[X_c]} \cdot \frac{R_g + [G_c] + U_g/D_i}{R_g + [G_c] - U_g/D_o} \quad (10a)$$

Making the substitution, $X = G$, and rearranging gives the following slope-intercept relation:

$$\frac{U_g((1/D_o + 1/D_i)U_{g-}/[G_c] - 1)}{U_{g+}/[G_e] - U_{g-}/[G_c]} = R_g - U_g \frac{1}{D_o} \quad (10b)$$

Fig. 4 shows the plot suggested by Eqn 10b. From the intercept and slope of the solid line we can make the approximation: $R_g \simeq 1.0 \text{ mM}$ and $1/D_o \simeq 0.010 \text{ min} \cdot \text{cell} \cdot \text{ml}^{-1}$. From these estimates we also have: $1/D_i \simeq 0.062 \text{ min} \cdot \text{cell}^{-1} \cdot \text{ml}^{-1}$ and $1/K_{go} + 1/K_{gi} = 1/R_g + 1/B_g \simeq 1.000 + 0.066 = 1.066 \text{ ml}/\mu\text{mole}$. These must be considered crude values, subject to revision; since they are based on separate sets of data obtained under slightly different conditions. They do, however, provide approximations sufficient for the next step in the analysis. The values will be revised essentially on the basis of Miller's data. The dot-dashed line corresponds to the revised values, its slope and intercept being within 20% of those of the solid line taken from Naftalin's data.

The crosses in this figure show the same plot with $1/D_o + 1/D_i$ assigned a zero value. It should be horizontal if this assignment were correct; for, in the absence of unstirred layers, both sides of Eqn 10b should be R_g under all conditions. It does not seem to be horizontal, and to the extent that it is not, this plot provides further evidence (independent of the sorbose data of Fig. 2) for the unstirred layer.

Glucose exit with various external glucose levels

If only glucose is present, Eqn 1 reduces to the following:

$$U_g = \frac{F_g((1/D_o + 1/D_i)U_{g-}/[G_c] - 1)}{1 + ([G_e] - U_g/D_o)/K_{go} + ([G_c] + U_g/D_i)/K_{gi} + ([G_e] - U_g/D_o)([G_c] + U_g/D_i)/R_g B_g} \quad (11)$$

This equation should fit Miller's exit data [8] shown in Fig. 3. It can be arranged (with substitutions from Eqn 6) in the following slope-intercept form:

$$\frac{F_g}{U_g} = \frac{1 + ([G_c] + U_g/D_i)/B_g}{[G_c] - [G_c] - (1/D_o + 1/D_i)U_g}$$

$$= \frac{1}{K_{go}} + \frac{([G_c] + U_g/D_i)(1 + ([G_c] - U_g/D_o)/B_g)}{[G_c] - [G_c] - (1/D_o + 1/D_i)U_g} \cdot \frac{1}{R_g} \quad (11a)$$

Fig. 5 shows the suggested plot. The solid line through the closed circles gives (or is compatible with): $K_{go} = 0.98$ mM and $R_g = 0.96$ mM. This value of R_g agrees rather well with that from Fig. 4. From Eqn 6, we now have $K_{gi} = 11.1$ mM. All glucose transport constants are thereby evaluated, and these constants are compatible with and in appropriate equations will predict the observed data used in their evaluation.

It should be noted that the Sen-Widdas net-transport data of Fig. 3 contain all the information needed to solve for $1/D_o$, $1/D_i$, R_g , K_{go} and K_{gi} (there being only three degrees of freedom in these five constants), once F_g , B_g and $1/D_o + 1/D_i$ were determined in Fig. 2. This would require 3-dimensional plot or trial and error

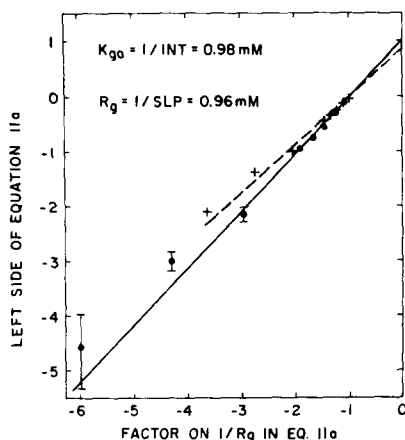
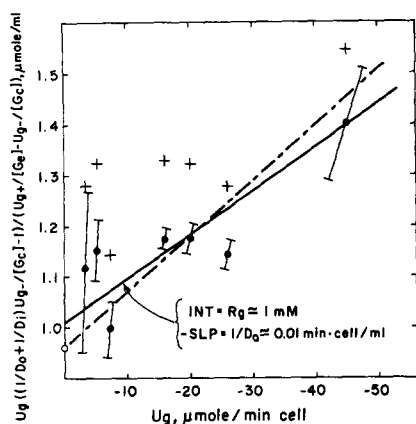


Fig. 4. Plot of flux data from Fig. 3. This plot is designed to determine the resistance ($1/D_o$) offered by the external unstirred layer and the flux-ratio constant (R_g) of glucose. The solid circles and solid line are based on the value of $1/D_o + 1/D_i$ obtained from sorbose and glucose resistance curves in Fig. 2. The solid line indicates: $1/D_o = 0.01 \text{ min} \cdot \text{cell}^{-1} \cdot \text{ml}^{-1}$ and $R_g = 1.0$ mM. The crosses are based on the assumption that $1/D_o + 1/D_i = 0$ (sorbose data ignored). The open circle on the Y axis is the value of R_g (0.96 mM) obtained from Fig. 5. The dot-dashed line has the slope corresponding to the $1/D_o$ value ($0.011 \text{ min} \cdot \text{cell}^{-1} \cdot \text{ml}^{-1}$) used to fit the glucose-galactose exchange experiment (presented later).

Fig. 5. Plot of glucose exit data from Fig. 3. This plot is designed to determine the Michaelis constant for glucose entry (K_{go}) and the flux-ratio constant (R_g) of glucose. The solid circles (●) and solid line are based on values of F_g , B_g , and $1/D_o + 1/D_i$ obtained from the sorbose and glucose resistance curves of Fig. 2 as well as the values of $1/D_o$ and $1/D_i$ obtained from Fig. 4. The crosses (+) and dashed line are based on the assumption that $1/D_o = 1/D_i = 0$, $F_g = 7.52 \text{ ml} \cdot \text{min}^{-1} \cdot \text{cell}^{-1}$, $B_g = 32.8$ mM (sorbose data ignored in the interpretation of glucose resistance curve of Fig. 2). It is not clear from this plot that the solid line is the best fit of the solid points. The constants corresponding to this line were used in Eqn 11 to generate the solid line in Fig. 3, where the adequacy of the fit can be seen more clearly. The dashed line fits the crosses equally well and agrees with the data of Fig. 3 equally well.

fitting. We did the latter before Naftalin published his efflux data and we obtained the best fit with essentially the constants shown here. Thus, had the flux-ratio approach given an incompatible value for $1/D_o$, we would not have obtained the precise fit of the net transport data of Fig. 3 (solid line), and the R_g of Fig. 5 would not have agreed with that of Fig. 4. The merit of the flux-ratio approach is that it excludes the denominator of Eqn 1 from consideration and allows one to proceed with 2-dimensional rectilinear plots. With only two degrees of freedom in each plot, the precision is improved.

The plot shown in crosses (+) was obtained without consideration of sorbose data and unstirred layers, i.e. with the values: $1/D_o + 1/D_i = 0$, $F_g = 7.52 \text{ ml} \cdot \text{min}^{-1} \cdot \text{cell}^{-1}$ and $B_g = 32.8 \text{ mM}$ (the naive interpretation of the glucose exchange data in Fig. 2). The dashed line through the crosses gives: $K_{go} = 1.17 \text{ mM}$, $R_g = 1.13 \text{ mM}$, and $K_{gi} = 17.2 \text{ mM}$. These three constants are, therefore, only moderately dependent on the interpretation of Fig. 2.

Galactose transport

According to the data* of Levine and Stein [18], the concentration of galactose at equilibrium which would inhibit sorbose transport 50% (double the resistance) at 20 °C should be something greater than 100 mM. Since unstirred layers are such a minor factor in sorbose transport, we can assume this to be a direct estimate of the B constant for galactose. If we let galactose be sugar S , then an approximation is $B_s = 110 \text{ mM}$.

According to Miller [8], the efflux of galactose, from cells exposed to 130 mM galactose on either side of the membrane, is $125 \mu\text{moles} \cdot \text{min}^{-1} \cdot \text{cell}^{-1}$. Knowing $1/D_o + 1/D_i = 0.072 \text{ min} \cdot \text{cell}^{-1} \cdot \text{ml}^{-1}$ and assuming $B_s = 110 \text{ mM}$, one can evaluate F_s by Eqn 9 to be $2.25 \text{ ml} \cdot \text{min}^{-1} \cdot \text{cell}^{-1}$.

A comparison of the definitions of F_g , F_s , R_g and R_s will show that

$$R_s F_s = R_g F_g \quad (12)$$

Thus, $R_s = 0.96 \cdot 16.4/2.25 = 7.0 \text{ mM}$. We now have $1/K_{so} + 1/K_{si} = 1/R_s + 1/B_s = 0.143 + 0.009 = 0.152 \text{ ml}/\mu\text{mole}$.

According to Miller [8], the exit of galactose, (from cells loaded with 130 mM galactose into sugar free medium) is $80 \mu\text{moles} \cdot \text{min}^{-1} \cdot \text{cell}^{-1}$. By Eqn 11a, K_{so} is evaluated at 7.23 mM. By Eqn 6a, $K_{si} = 71 \text{ mM}$.

The same evaluations with the sorbose data of Fig. 2 ignored ($1/D_o + 1/D_i = 0$) give the following: $F_s = 2.10 \text{ ml} \cdot \text{min}^{-1} \cdot \text{cell}^{-1}$, $R_s = 4.07 \text{ mM}$, $K_{so} = 4.18 \text{ mM}$, $K_{si} = 65.3 \text{ mM}$.

Effect of external galactose on glucose efflux

Miller [8] observed that the addition of 130 mM galactose to the outside of cells loaded with 130 mM glucose increased the glucose efflux from 100 to 250 $\mu\text{moles} \cdot \text{min}^{-1} \cdot \text{cell}^{-1}$. If the constants that have now been evaluated for glucose and galactose transport are correct then they should predict this effect when inserted into

* Miller's [8] optical measurements of sorbose transport in the presence of glucose, galactose or mannose at equilibrium are uninterpretable, owing to the counter movements of the inhibitory sugars. The tracer measurements of Stein's group are not subject to this criticism.

Eqn 1. Since rates U_g and U_s appear in the argument, this requires alternately evaluating U_s and U_g five times, i.e. until these evaluations stop changing. When this is done (with the constants deriving from the sorbose data of Fig. 2, hence, with the unstirred layers in the picture), glucose transport calculates to be $U_g = -220 \mu\text{moles} \cdot \text{min}^{-1} \cdot \text{cell}^{-1}$, and galactose transport calculates to be $U_s = 210 \mu\text{moles} \cdot \text{min}^{-1} \cdot \text{cell}^{-1}$. The carrier hypothesis with unstirred layers, therefore, predicts the surprising fact that external galactose enhances glucose efflux more than external glucose enhances glucose efflux ($197 \mu\text{moles} \cdot \text{min}^{-1} \cdot \text{cell}^{-1}$) and more than external galactose enhances galactose efflux ($125 \mu\text{moles} \cdot \text{min}^{-1} \cdot \text{cell}^{-1}$). Miller observed a slightly larger enhancement. The agreement can be greatly improved by a modest adjustment of $1/D_o$, the least reliable of the constants. If $1/D_o$ is increased from $0.010 \text{ min} \cdot \text{cell} \cdot \text{ml}^{-1}$ to $0.011 \text{ min} \cdot \text{cell} \cdot \text{ml}^{-1}$ (the dot-dash line in Fig. 4) and all the constants depending on its value appropriately adjusted, the following values are obtained: $1/D_i = 0.061 \text{ min} \cdot \text{cell} \cdot \text{ml}^{-1}$, $K_{go} = 0.975 \text{ mM}$, $K_{gi} = 12.13 \text{ mM}$, $K_{so} = 7.22 \text{ mM}$, and $K_{si} = 72.4 \text{ mM}$ — other constants remaining the same. Glucose–galactose exchange then calculates: $U_g = -233 \mu\text{moles} \cdot \text{min}^{-1} \cdot \text{cell}^{-1}$ and $U_s = 223 \mu\text{moles} \cdot \text{min}^{-1} \cdot \text{cell}^{-1}$. This is within the standard error reported by Miller*. The interaction between external galactose and internal glucose, therefore, provides an estimation of $1/D_o$ (and the other adjusted constants) independent of Fig. 4.

It should be pointed out that these conclusions are little dependent on the value placed on B_s at the outset of the analysis of galactose transport. Originally we used a value $B_s = 40 \text{ mM}$ (accepting Miller's data, at face value) and obtained the prediction that external galactose would promote glucose efflux to the surprising degree observed by Miller.

If the sorbose data are ignored and hence unstirred layers not taken into account, the expected glucose efflux into galactose medium is calculated to be only $171 \mu\text{moles} \cdot \text{min}^{-1} \cdot \text{cell}^{-1}$. However, a greater enhancement can be expected if the galactose exit and exchange data are adjusted within their standard errors. If one assumes that galactose exchange in cells equilibrated with 130 mM galactose was $133 \mu\text{moles} \cdot \text{min}^{-1} \cdot \text{cell}^{-1}$ and galactose exit into empty medium was $74 \mu\text{moles} \cdot \text{min}^{-1} \cdot \text{cell}^{-1}$, then the galactose constants would be $B_s = 110 \text{ mM}$, $F_s = 2.23 \text{ ml} \cdot \text{min}^{-1} \cdot \text{cell}^{-1}$, $R_s = 3.83 \text{ mM}$, $K_{so} = 3.98 \text{ mM}$, and $K_{si} = 52 \text{ mM}$. With 130 mM glucose inside and 130 mM galactose outside, $U_g = -233 \mu\text{moles} \cdot \text{min}^{-1} \cdot \text{cell}^{-1}$ and $U_s = 229 \mu\text{moles} \cdot \text{min}^{-1} \cdot \text{cell}^{-1}$, which is now within the standard error of the rate reported by Miller. The fact that a large distortion of the galactose transport data is needed to predict the effect of galactose on glucose efflux when unstirred layers are not included in the analysis, suggests again that unstirred layers are a reality.

* An adjustment to $1/D_o = 0.012 \text{ min} \cdot \text{cell} \cdot \text{ml}^{-1}$ would have given $U_g = -249 \mu\text{moles} \cdot \text{min}^{-1} \cdot \text{cell}^{-1}$. We elected not to make the fitting so perfect, since Eilam and Stein [17] show that the distinction between [^{14}C]glucose–glucose exchange and [^{14}C]glucose–galactose exchange may have been slightly overestimated by Miller. We judge from their paper [17] that the distinction certainly did exist at the very beginning of the exchange.

DISCUSSION

Models

The central conclusion of this work is that all of the anomalies observed by Miller in 1968 were explicable in terms of the unsimplified carrier model [5] described in 1964 together with the unstirred layers which Miller considered at the time [9]. Other models [13–16] have not been shown to accommodate all these data with a single set of constants. For example, the tetramer model of Lieb and Stein [13] did not predict the surprisingly large enhancement of glucose efflux by external galactose. The lattice model of Naftalin [14] was not tested for its ability to fit the various experimental data with a single set of constants. The introversion model of LeFevre [16] predicts that low concentrations of glucose should promote sorbose transport, contrary to observations. Moreover, the glucose exchange experiment of Miller [8] appeared not to be accommodated. Geck's asymmetrical carrier [11] without unstirred layers failed to reconcile the difference between the K_m for glucose exchange and the K_i for inhibition of sorbose transport by glucose. In addition, the present analysis shows that unstirred layers are needed with the asymmetric carrier to explain the effect of external galactose on glucose efflux (and, if one accepts the data, the fact that apparent R_g increased with U_g in Fig. 4).

Hankins and Stein [20] found that mixing of well dispersed cells did not affect glucose exit appreciably, and they argued that the dependency of exit on stirring observed by Naftalin [10] was due to cell cohesion in his poorly stirred suspensions. Miller [19] has argued that his cells were well dispersed and that diffusion distances outside his cells were too short for diffusion to limit distribution in the bulk medium. He did not rule out transitory cohesions of cells at their concave surfaces as contributing to the external unstirred layer revealed kinetically. However, the main diffusion barrier seems to be at the internal surface where diffusion distances are short indeed. We, therefore, do not think of the unstirred layers as reflecting diffusion through the bulk aqueous phases. Instead, we suggest that the carrier loads and unloads somewhere beneath the outermost membrane structures, and these structures hinder the movement of sugar between bulk phases and the loading–unloading points. These structures might be proteins, glycolipids, phospholipids or all of these, forming a densely packed layer especially at the inner surface. Some of the water in this layer may be somewhat immobile owing to hydrogen bonding. Considered in these terms, the unstirred layer may be an interesting property of the membrane deserving further characterization. One of the journal reviewers informed us of a recent article by Wilbrandt [21] in which he drew precisely these conclusions, based on data of his own laboratory. His estimate of $1/D_o + 1/D_i$ was 0.05 of which 10% might be $1/D_o$. Although he did not put dimensions on the number, his explanation indicates that it is comparable to our $0.072 \text{ min} \cdot \text{cell} \cdot \text{ml}^{-1}$.

We have omitted attempts to fit Miller's glucose counterflow experiment [8], which he considered incompatible with the carrier hypothesis with or without unstirred layers. Our analysis of that experiment, based on considerations quite independent of any model, leads us to the conclusion that the incompatibility was due to experimental error, as suggested by Lieb and Stein [13].

Experimental design

According to the model in Fig. 1, glucose transport in human erythrocytes can be characterized by 6 constants, F_g , B_g , R_g , K_{g0} , D_o and D_i . A seventh, K_{gi} , can be derived from others. The inhibitory effect of glucose at equilibrium on the transport of a low affinity sugar at low concentration plays a big role in assessment of the unstirred-layer effect. Although sorbose seems to be appropriate for this experiment in human erythrocytes, it may not be for other cells containing a separate fructose-transport system [5]. Allose is probably a better choice in general. By use of double labelling, glucose exchange and low-affinity sugar transport could be measured simultaneously, so that one may be quite sure of the difference in resistance-doubling glucose concentration (see Fig. 2) giving rise to the estimation of $1/D_o + 1/D_i$, as well as F_g , B_g and F_x . Moreover, experiments of the Sen-Widdas type should be accompanied by simultaneous efflux measurements by use of double labelling.

Given the conclusion that the model of Fig. 1 explains adequately the glucose transport data, one can in principal determine all constants from five experimental runs: (1a) Efflux of [^{14}C]glucose and [^3H]allose from cells containing these two sugars at about 0.1 mM in a medium containing these two sugars unlabelled at 0.1 mM. (1b) Efflux of [^{14}C]glucose and [^3H]allose from cells containing glucose at 100 mM and allose at 0.1 mM into a medium containing unlabelled glucose at 100 mM and unlabelled allose at 0.1 mM. (2a) Exit of [^{14}C] glucose and [^3H]glucose from cells loaded with glucose at 100 $\mu\text{moles/cell}$ into medium containing no sugar (the double label serves no purpose except to demonstrate agreement between the two labels). (2b) Exit of [^{14}C]glucose and efflux of [^3H]glucose from cells loaded with glucose at 100 $\mu\text{moles/cell}$ into medium containing [^{14}C]glucose (same specific activity) at 2 mM. (2c) Like 2b with 10 mM [^{14}C]glucose in medium. Tests 1a and 1b can be analyzed as was Fig. 2, while tests 2a, 2b and 2c can be analyzed as were Figs 3, 4 and 5. Hence, all the constants would be evaluated. This abbreviated series of tests is suggested for surveys of temperature or pH dependency or for any graded response study. Also, other high-affinity sugars could be substituted for glucose to provide a preliminary test of Eqn 12 and of the unstirred layer hypothesis, inasmuch as the model predicts that all sugars will show the same values for $F_x R_x$, D_o and D_i . A more rigorous analysis of a given sugar under a given condition would involve extension of 1b to other concentrations, extension of 2a to other cellular sugar concentrations, extension of 2b and 2c to other external concentrations, as well as studies of sugar entry into empty cells from medium with various sugar concentrations. All measurements of net transport should be plotted as described for Fig. 5. If the net entry and net exit experiments form a single straight line, then this will constitute a confirmation of Eqns 6 and 11, for this plot (Eqn 11a) depends on Eqn 6 as well as Eqn 11.

Rejection criteria

Recent discussions [23, 24] have been concerned with "rejection criteria", i.e. experimental observations incompatible with the carrier hypothesis. Those so far published are essentially Eqns 11 (with $1/D_o = 1/D_i = 0$) and 6 together. Thus, if one were to determine the four constants of Eqn 6 independently and prove that Eqn 6 could not be satisfied, then the carrier hypothesis would have to be rejected. We suspect that some of the published criteria may be in error. For example, the last denominator term in Hoare's [24] equation probably should be negative.

According to our symbolism, the Sen-Widdas K_m should be $R_g B_g / K_{gi}$, which is $B_g / (1 + K_{gi} / K_{go} - K_{gi} / B_g)$, an expression equivalent to Hoare's, except for the sign on K_{gi} / B_g . Unfortunately, the Sen-Widdas K_m has no theoretical meaning in a system with unstirred layers, for, the Sen-Widdas experiment must in this case be analyzed according to Fig. 5. The various slope-intercept plots suggested here (Eqns 9b, 10b, 11a) are also rejection criteria, since the carrier hypothesis predicts straight lines. In fact such straight lines preclude some other rejection criteria [23], inasmuch as the equations involved account for all transmembrane effects. Eqn 12 is a rejection criterion which is somewhat independent of the others and should be seriously tested. Hankin, et al. [23] reported a time course of glucose uptake which they claimed to be incompatible with the carrier hypothesis. However, their experiment was conceptually similar to one carried out by Lacko et al. [12], whose data entirely compatible with the carrier hypothesis [11]. Hence, the incompatible time course [23] must be questioned. A modest error in washing out or subtracting extracellular glucose would affect the conclusions seriously. Possibly, unstirred layers would provide an explanation for the anomalous time course [23], but we have not attempted to check this.

In interpreting data apparently incompatible with the carrier model, one should consider the possibility that glucose enters by more than one process, one with high and one with low affinity [5, 22]. Data which can be interpreted in this way do not justify rejection of the carrier hypothesis.

Interpretation of transport constants

The interactions of glucose and the carrier are characterized by an activity constant (F_g) plus four dissociation-like constants (K_{go} , K_{gi} , R_g and B_g) which are related to each other such that any three of these define the fourth. Hence, there are four "independent" constants in all. As seen in the definitions of these constants, each of them is a complex function of rate constants for several events in the carrier cycle. However, there are ways that the empirical constants can be put together so as to cancel several components, leaving simpler relations. The V expressions are examples of this:

V for glucose entry

$$= F_g K_{go} = C_i / (1/k_{23} + 1/k_4) = 16.0 \mu\text{moles} \cdot \text{min}^{-1} \cdot \text{cell}^{-1}, \quad (13)$$

V for glucose exit

$$= F_g K_{gi} = C_i / (1/k_{-21} + 1/k_{-4}) = 199 \mu\text{moles} \cdot \text{min}^{-1} \cdot \text{cell}^{-1}, \quad (14)$$

V for glucose exchange

$$= F_g B_g = C_i / (1/k_{23} + 1/k_{-21}) = 247 \mu\text{moles} \cdot \text{min}^{-1} \cdot \text{cell}^{-1}, \quad (15)$$

V for free-carrier exchange

$$= F_g R_g = C_i / (1/k_4 + 1/k_{-4}) = 15.7 \mu\text{moles} \cdot \text{min}^{-1} \cdot \text{cell}^{-1} \quad (16)$$

One can see that the reciprocal rate constants in each denominator are series resistances as pointed out by Geck [11]. These relations show that k_4 is much less than any of the other mobilities or translocation constants. It is this low value of k_4 which makes maximal entry slow relative to maximal glucose exchange (or exit) and, therefore, predicts the observation [12] that internal glucose can promote glucose influx

more than 10-fold. From the above relations, it is seen that another set of simplifications is obtained from ratios among the dissociation-like constants:

$$K_{go}/R_g = (1/k_4 + 1/k_{-4})/(1/k_{23} + 1/k_4) = (1 + k_4/k_{-4})/(1 + k_4/k_{23}) \quad (17)$$

$$K_{gi}/R_g = (1/k_4 + 1/k_{-4})/(1/k_{-21} + 1/k_{-4}) = (1 + k_{-4}/k_4)/(1 + k_{-4}/k_{-21}) \quad (18)$$

$$K_{go}/B_g = (1/k_{23} + 1/k_{-21})/(1/k_{23} + 1/k_4) = (1 + k_{23}/k_{-21})/(1 + k_{23}/k_4) \quad (19)$$

$$K_{gi}/B_g = (1/k_{23} + 1/k_{-21})/(1/k_{-21} + 1/k_{-4}) = (1 + k_{-21}/k_{23})/(1 + k_{-21}/k_{-4}) \quad (20)$$

Although we do not believe that the Sen-Widdas K_m can be obtained accurately in a system with unstirred layers, it should nevertheless be noted that the hypothetical Sen-Widdas K_m , i.e. $R_g B_g / K_{gi}$, divided into B_g gives K_{gi}/R_g and divided into R_g gives K_{gi}/B_g . With these relations one can solve for any one ratio (e.g. k_{23}/k_4) as a function of another ratio (e.g. k_{-4}/k_4) and show the possible simultaneous values of both:

$$k_{23}/k_4 = (K_{go}/R_g)/(1 - K_{go}/R_g + 1/(k_{-4}/k_4)) \quad (21)$$

$$k_{-21}/k_4 = (K_{gi}/R_g)/(1 + (1 - K_{gi}/R_g)/(k_{-4}/k_4)) \quad (22)$$

With these values, all other simultaneous ratios can be obtained, e.g. k_{23}/k_{-21} , k_{23}/k_{-4} and k_{-21}/k_{-4} . With such values then, the possible simultaneous "true dissociation constants" can be calculated from rearrangements of the definitions of K_{go} and K_{gi} :

$$(k_{-1} + k_{23})/k_1 = K_{go}(1 + k_{23}/k_4)/(1 + k_{-4}/k_4) \quad (23)$$

$$(k_3 + k_{-21})/k_{-3} = K_{gi}(1 + k_{-21}/k_{-4})/(1 + k_{-4}/k_4) \quad (24)$$

These are all shown in Fig. 6 as functions of k_{-4}/k_4 . Owing to the vertical asymptotes of these relations (beyond which impossible negative values occur), we can place the following approximate limits on these ratios:

$$11 < k_{-4}/k_4 < 64; k_{23}/k_4 > 14; k_{-21}/k_4 > 15.$$

Thus, the outward movement of free carrier occurs with great difficulty relative to the inward movement of free carrier and the movement of glucose-loaded carrier in either direction; i.e. free carrier at the inside is in a much more stable state than free carrier on the outside or loaded carrier on either side, and in the absence of sugar at least 90% of the carrier will be on the inside. (When no sugar is present $U_g = U_s = 0 = C_i k_4 - C_o k_{-4}$; hence $C_i k_4 = C_o k_{-4}$; and $C_i/C_o = k_{-4}/k_4$). One can imagine a variety of conceptually similar mechanisms by which C_i might be stabilized.

If one supposes that the carrier inherently prefers to be on the inside, then the vertical dotted line near the right hand limit of Fig. 6 would be an appropriate place to examine the functions. On that line, $k_{-4}/k_4 \simeq 60$ and $k_{23}/k_{-21} \simeq 64$; hence, the loaded and unloaded carrier both greatly prefer the inside. Also $k_{23}/k_{-4} \simeq 15.7$ and $k_{-21}/k_4 \simeq 15.7$; hence, the addition of sugar to the carrier on either side enhances mobility about 16-fold. The increased mobility would probably represent the conformational effect of sugar already postulated to explain the fact that sugars promote carrier inactivation by 1-fluoro-2,4-dinitrobenzene to a degree depending on the sugar affinity or structure as well as the fraction of carrier occupied by sugar [25, 26]. Note that under this circumstance, the true dissociation constants must be the same on both sides of the membrane.

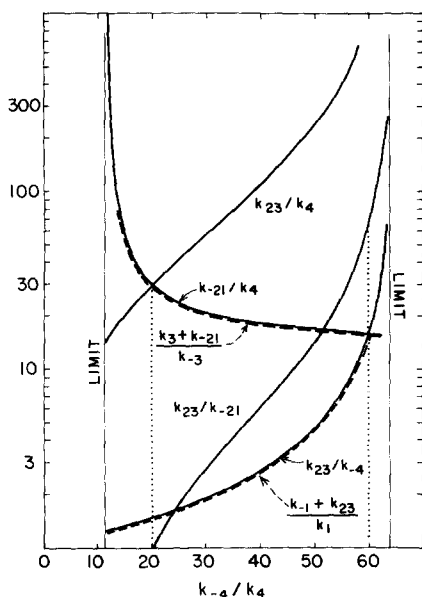


Fig. 6. Reaction-constant ratios calculated from empirical transport constants. The text describes the equations for these lines. Any vertical line between the limits will cross the abscissa and the curves at compatible points. The dashed lines are the true dissociation constant $(k_{-1} + k_{23})/k_1$ and $(k_3 + k_{-21})/k_{-3}$ which happen to parallel closely the ratios k_{23}/k_{-4} and k_{-21}/k_4 , respectively (— — —)

However, it is also possible that the carrier is inherently symmetrical in its behavior and that the asymmetry is due to a non-transportable competitive inhibitor present at the inside surface of the cell but essentially absent at the outside. Such a substance, by preventing glucose collisions and mobility (when bound) would seem to lower k_4 and k_{-3} by a common factor, thereby lowering F_g and raising K_{gi} and B_g simultaneously (see definitions of these constants). The inhibitor would have to be tightly membrane bound, since LeFevre [27] failed to see any increase of glucose transport when erythrocytes were depleted of protein. The vertical dotted line near the left-hand limit of Fig. 6 is compatible with this view. On this line, $k_{23}/k_4 = k_{-21}/k_4 = 30$, i.e. the loaded carrier moves with equal facility in either direction. Also, on this line, $k_{-4}/k_4 = 20$, i.e. the free carrier moves inward almost as readily as the loaded carrier in either direction. The only markedly peculiar mobility, then, is the outward movement of free carrier, k_4 ; and this could be low, not because the free carrier has difficulty making this move, but because most of the sugar-free carrier at the inner surface is bound to a non-transportable competitive inhibitor. Note that differences in true dissociation constants, $(k_{-1} + k_{23})/k_1$ vs $(k_3 + k_{-21})/k_{-3}$, in this case account entirely for differences between K_{go} and K_{gi} . The present kinetic analysis favours this view, since a plot of analogous ratios (k_{67}/k_4 and k_{-65}/k_4) based on the galactose constants shows an upper limit with $k_{-4}/k_4 \simeq 30$. If this, as well as the glucose constants, are borne out by future data, then the true value of k_{-4}/k_4 cannot be far from the left-hand vertical dotted line. According to this view, one might interpret Krupka's observations to suggest that the endogenous competitive inhibitor protects the carrier from 1-fluoro-2,4-dinitrobenzene as does maltose,

possibly by holding it in a hydrophilic location, glucose having the opposite effect possible by increasing the exposure in the hydrophobic layer. The non-transportable competitive inhibitor provides an explanation of the paradoxical fact that the "apparent dissociation constant", B_g , is either temperature-insensitive [12] or decreases with higher temperature [18], while other dissociation-like constants such as K_{go} (ref. 12) or the Sen-Widdas K_m (ref. 28), $R_g B_g / K_{gi}$, show the expected increase with higher temperature. If the sugar-free carrier on the inside is bound by a non-transportable competitive inhibitor, then B_g (and K_{gi}) is high due to the inhibitor and, as temperature rises, the inhibitor dissociation constant rises, thereby reducing the tendency for the inhibitor to raise B_g (and K_{gi}). The inherently asymmetric carrier would not seem to explain the peculiar temperature effect on B_g , inasmuch as all denominator constants would be expected to increase with temperature.

ACKNOWLEDGEMENTS

This research was supported by U.S.P.H.S. Program Grant No. 5 P01 AM-07462 and Vanderbilt University Diabetes-Endocrinology Center AM-17026.

REFERENCES

- 1 Widdas, W. F. (1952) *J. Physiol.* 118, 23-39
- 2 Rosenberg, Th. and Wilbrandt, W. (1955) *Exp. Cell Res.* 9, 49-67
- 3 Wilbrandt, W., Frei, S. and Rosenberg, Th. (1956) *Exp. Cell Res.* 11, 59-66
- 4 Bowyer, F. and Widdas, W. F. (1958) *J. Physiol.* 141, 219-232
- 5 Regen, D. M. and Morgan, H. E. (1964) *Biochim. Biophys. Acta* 79, 151-166
- 6 Levine, M., Oxender, D. L. and Stein, W. D. (1965) *Biochim. Biophys. Acta* 109, 151-163
- 7 Mawe, R. C. and Hempling, H. G. (1965) *J. Cell Comp. Physiol.* 66, 95-103
- 8 Miller, D. M. (1968) *Biophys. J.* 8, 1329-1338
- 9 Miller, D. M. (1968) *Biophys. J.* 8, 1339-1352
- 10 Naftalin, R. J. (1971) *Biochim. Biophys. Acta* 233, 635-643
- 11 Geck, P. (1971) *Biochim. Biophys. Acta* 241, 462-472
- 12 Lacko, L., Wittke, B. and Kromphardt, H. (1972) *Eur. J. Biochem.* 25, 447-454
- 13 Lieb, W. R. and Stein, W. D. (1970) *Biophys. J.* 10, 585-609
- 14 Naftalin, R. J. (1970) *Biochim. Biophys. Acta* 211, 65-78
- 15 Lieb, W. R. and Stein, W. D. (1972) *Biochim. Biophys. Acta* 265, 178-207
- 16 LeFevre, P. G. (1973) *J. Membrane Biol.* 11, 1-19
- 17 Eilam, Y. and Stein, W. D. (1972) *Biochim. Biophys. Acta* 266, 161-173
- 18 Levine, M. and Stein, W. D. (1966) *Biochim. Biophys. Acta* 127, 179-193
- 19 Miller, D. M. (1972) *Biochim. Biophys. Acta* 266, 85-90
- 20 Hankin, B. L. and Stein, W. D. (1972) *Biochim. Biophys. Acta* 288, 127-136
- 21 Wilbrandt, W. (1972) *Biomembranes* 3, 79-99
- 22 Hoos, R. T., Tarpley, H. L. and Regen, D. M. (1972) *Biochim. Biophys. Acta* 266, 174-181
- 23 Hankin, B. L., Lieb, W. R. and Stein, W. D. (1972) *Biochim. Biophys. Acta* 288, 114-126
- 24 Hoare, D. G. (1972) *Biochem. J.* 127, 62p
- 25 Krupka, R. M. (1971) *Biochemistry* 10, 1143-1153
- 26 Krupka, R. M. (1972) *Biochim. Biophys. Acta* 282, 326-336
- 27 LeFevre, P. G. (1961) *Nature* 191, 970-972
- 28 Bolis, L., Luly, P., Pethica, B. A. and Wilbrandt, W. (1970) *J. Membrane Biol.* 3, 83-92